

Trim and water surface deformation under the cushion

5.1 Introduction

Dynamic trim is determined by equilibrium of the steady forces acting on the ACV or SES at speed. The trim will affect drag forces acting on the craft and therefore its ability to accelerate through hump speed to the operational cruising speed. The main purpose of this chapter's investigation is therefore to enable estimation of craft trim at various speeds and identify the optimum values.

The starting point for determination of equilibrium is the centre of pressure of the cushion for an ACV and in addition the force vector which results from the hydrodynamic force acting on the hulls of an SES or through the skirt. This may be compared with the forces acting on the hull of a planing boat or catamaran.

An important difference from conventional ships regarding determination of the hydrodynamic force and moment is caused by the inner water surface under the pressurized cushion. Conventional ships have only an outer draft, while the ACV and SES have both inner and outer drafts. The inner water surface profile is very difficult to observe, though a number of model experiments have been carried out to verify analytical models developed using classical hydrodynamic theory in the 1960s and these have largely confirmed analysis.

The SES has water propellers or water jets and other underwater appendages which will affect its dynamic trim in a similar way to a fast planing craft. The amphibious ACV on the other hand normally has air propellers or fans which induce pitching moments and fins and elevators or elevons to control dynamic trim. The ACV and SES are also both affected by the trimming moments from aerodynamic drag and lift of the hull and superstructure above the water profile.

Considering first the dynamic equilibrium of the cushion itself, the craft dynamic trim, including inner and outer drafts and trim angle, is influenced by a number of design and performance parameters of the craft as follows.

Trim

Trim is influenced by many cushion characteristic parameters, for example:

- position of cushion LCP;
- bow/stern skirt clearance (air gap) over the base line;
- cushion pressure ratio of air supply from lift fans and thus skirt stiffness;
- position of LCG based on distribution of craft mass, payload and ballast;
- position of the thrust line and thus dynamic trimming moments.

Bow and stern seal interaction

The inner water surface at bow and stern seals will influence skirt drag and trimming moment, particularly in the case of craft take-off through hump speed.

Wetted surfaces

The geometry of inner/outer water surfaces will directly influence wetted surface and friction drag of sidewalls (SES) and side skirts (ACV).

Location of SES inlets and appendages

The design and location of water-jet propulsion inlets, cooling water inlets, propellers, rudders and stabilizer fins, are all influenced by the shape of the inner/outer water surface. At the same time all of these items introduce thrust or drag forces affecting the craft's dynamic trim.

Some early SES projects at MARIC suffered a lot from imperfect selection of water-jet inlet locations. The water-jet propulsion inlet of SES model 717 and water-cooling pump of SES model 713 were not ideally positioned when first built. Due to lack of knowledge about the inner/outer water surface shape, MARIC located the inlet of the water-cooling pump of SES 713 inside the air cushion and the inlet of water-jet propulsion of SES 717 at the outer wall of the sidewalls. Air was ingested into the inlet of both these systems in the course of take-off through hump speed.

On SES model 713, the air ingesting into the cooling water pump led to air blockage of the system and interrupted the circulation of the cooling water. Thus the temperature of cooling water rose rapidly, sometimes up to 95°C, which was very dangerous for the engines. As for SES model 717 with water-jet propulsion, the craft sometimes did not pass through hump speed due to air ingestion into the water-jet pump, decreasing thrust. Both these problems almost became stumbling blocks for SES development in their early phase of research in China, arising from lack of knowledge concerning the dynamic trim of ACV/SES.

Figure 5.1 shows a picture of the inner and outer draft of model sidewalls taken from a towing tank model. Figure 5.2 shows the deformed water surface inside the craft cushion, obtained by the theoretical calculation. It may be noticed that a large hollow in the water surface at the rear and centre parts of the cushion occurs at Froude numbers close to 'hump speed', the transition between displacement mode and planing mode of operation. It is this that caused the air ingestion which happened

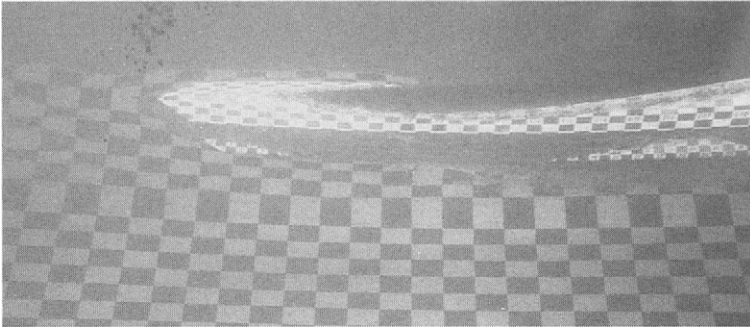


Fig. 5.1 Picture showing water surface deformation in/off cushion during model tests in towing tank.

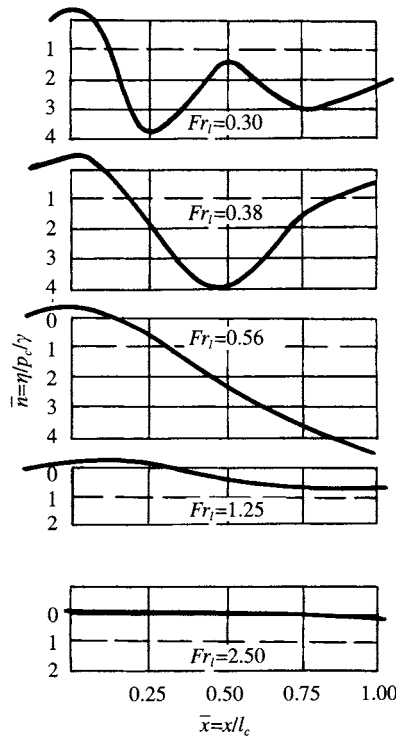


Fig. 5.2 Wave profile inside a cushion at various Froude numbers.

on early SES in China, for example, the air ingestion into the water cooling pump in SES model 713 and into the water propulsion system for model 717 and WD-901.

The depth of the wave hollow inside the cushion is equal to four times the cushion pressure depression, i.e. $\bar{n} = \eta [p_c / \gamma] \cong -4$ where η denotes wave hollow depth inside the cushion, p_c , the cushion pressure (N/m^2) and γ the weight density of water (N/m^3 , $\gamma = \rho_w g$, where ρ_w is normally taken as 998.4 kg/m^3 at 20°C and g as 9.81 m/s^2). Once the overall craft trim has been estimated at primary hump speed, it may therefore be

necessary to adjust the sidewall lines over the stern half of the vessel to ensure intakes and propellers stay fully immersed.

Internal stability skirts

The design of longitudinal and/or transverse stability skirts inside the cushion of an ACV strongly affects dynamic trim. The deeper these skirts, the larger the water drag, due to skirt wetting in the complex internal cushion wave pattern. The shallower these skirts are, the less effective they are. Determination of the optimum for a particular craft is only practical through parametric model tests in a towing tank, or trial and error with a prototype, which is likely to be rather more expensive.

Basic concepts for design

Misunderstanding of some basic concepts may lead to incorrect choices being made for craft design, trials and analysis. For example:

- Does the trim characterized by outer drafts of the craft at bow and stern represent the apparent or real trim angle of the craft?
- What is the relation between the trim angle formed by the outer water surface and the trim angle formed by the inner water-line?
- Is the craft's trim drag defined by the trim angle at the outer or inner water-line?
- What is the relation between the trim drag and wave slope induced by moving cushion pressure?

These problems are not immediately obvious without some practical experience of ACV behaviour and in some cases have been inaccurately described in the technical literature.

It can be seen that determination of ACV dynamic trim at different speeds is somewhat complicated and should be carefully dealt with during the design process. Based on a clear understanding of the basic concepts, one can solve the design problem by the method of initial predictions using theoretical analysis, later correlated with experimental testing.

In order to understand the interaction of craft dynamic trim with the cushion inner water surface, the water surface inside the cushion can be observed either by periscope in a model test [52], or by direct observation via a transparent window on a craft sidewall. This has been carried out in SES model 713. The outer water surface can be determined by photos as shown in Fig. 5.1.

5.2 Water surface deformation in/beyond ACV air cushion over calm water

ACV moving over deep water

When an ACV hovers statically on water, a depression will be formed between the inner and outer water surface, the depth of which will be

$$\eta = -p_c/\gamma$$

where η is the depth of depression, upward positive.

In the case of a craft moving over a water surface, the dynamic deformation of the water surface caused by the ACV has to be determined. According to linear water wave theory, when an air cushion with the length of L , beam of b and pressure distribution of $p(x,y)$ running on the free surface of calm water with the depth of H at constant speed of c , the disturbance velocity potential can be written by [53]

$$\phi = \frac{-i}{4\pi c \rho_w} \int_{-\pi}^{\pi} \sec \theta \int_0^{\infty} AB \, dk \int_{-\infty}^{\infty} C \, dm \, dn \quad (5.1)$$

where

$$A = \frac{e^{ik(x \cos \theta + y \sin \theta)}}{k - [g/c^2] \tanh kH (\sec \theta)^2 + i \mu/c \sec \theta}$$

$$B = \frac{\cosh k(H + z)}{\cosh kH}$$

$$C = p(m,n) e^{ik(m \cos \theta + n \sin \theta)}$$

and c is the moving velocity of the cushion (m/s), H the water depth (m), m,n any given variate, g the acceleration of gravity (9.81 m/s^2), ρ_w the water density (kg/m^3), (sea water 1021 at 20°C , fresh water 998.2 at 20°C), r the aspect ratio of the air cushion, $r = b_c/l_c$ and μ the dynamic viscosity coefficient (Ns/m^2) (1.3 at 10°C , 1.009 at 20°C , 0.8 at 30°C).

Assuming the pressure of the rectangular air cushion to be uniformly distributed, then the exciting disturbance potential can be written as

$$\phi = \frac{ip_c}{\pi^2 c \rho_w} \int_{-\pi}^{\pi} \sec \theta \, d\theta \int_0^{\infty} DBEF \, k \, dk \quad (5.2)$$

where

$$D = \frac{e^{-ik(x \cos \theta + y \sin \theta)}}{k - [g/c^2] (\sec \theta)^2 \tanh kH + i \mu/c \sec \theta}$$

$$E = \frac{\sin(kl \cos \theta)}{k^2 \cos \theta \sin \theta}$$

$$F = \frac{\sin(krl \cos \theta)}{k^2 \cos \theta \sin \theta}$$

Thus, the water surface deformation should meet the relation

$$\eta = \frac{l}{c} \left[\frac{\partial \theta}{\partial x} \right]_{x=0} - \frac{p_c}{\gamma} \quad (5.3)$$

where x, y, z form the perpendicular coordinates, x denotes the direction of air cushion movement and forward positive z denotes the vertical coordinate, upward positive.

The water surface deformation caused as the air cushion with uniformly distributed pressure moves forward may be defined by equations (5.2) and (5.3).

To determine the actual water surface profile, one has to take into account both the depression of the water surface induced by the air cushion hovering statically over the water and the water surface deformation caused by the air cushion moving on the water, i.e. the ratio between the x direction component of disturbing velocity on the free surface and its forward velocity.

Calculated results are shown in Fig. 5.3, where it can be seen that the water surface deformations will be rather different between in and beyond the cushion, and are a function of Froude number. Figs 5.4–5.6 show calculation results selected from ref. 54. They can be compared as follows:

1. From Fig. 5.4, it is found that the bow wave amplitude in the cushion is equal to that beyond the cushion. At high values of Fr_1 the bow water surface deformation both in the cushion and also beyond the cushion decreases so as to keep the same value. This agrees with test results.

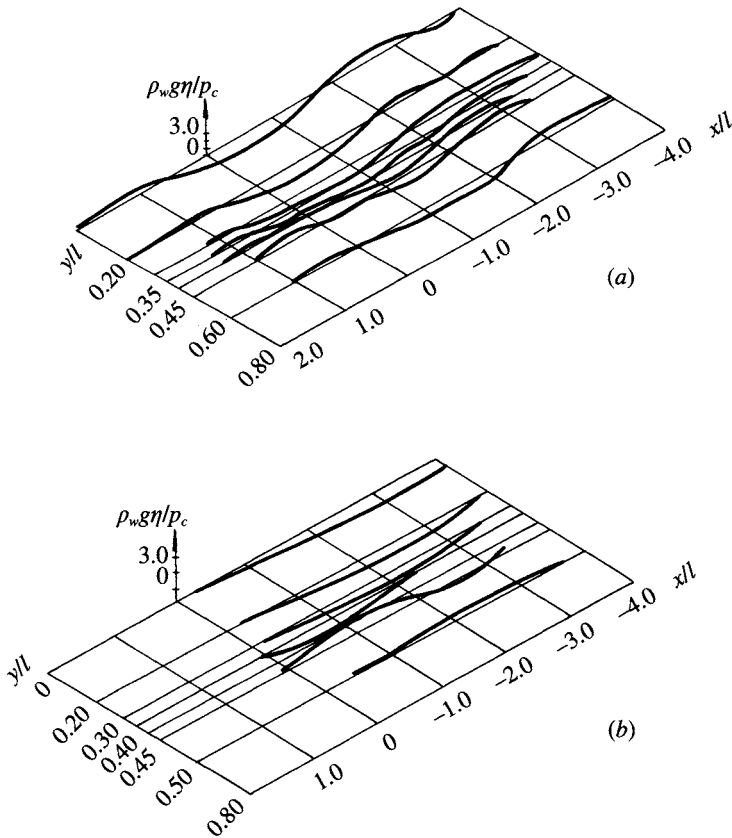


Fig. 5.3 Water surface deformation due to a moving air cushion pressure distribution $b/l = r = 0.4$: (a) vertical displacement of free water surface at $Fr = 0.9$, (b) vertical displacement of free water surface at $Fr = 3.0$.

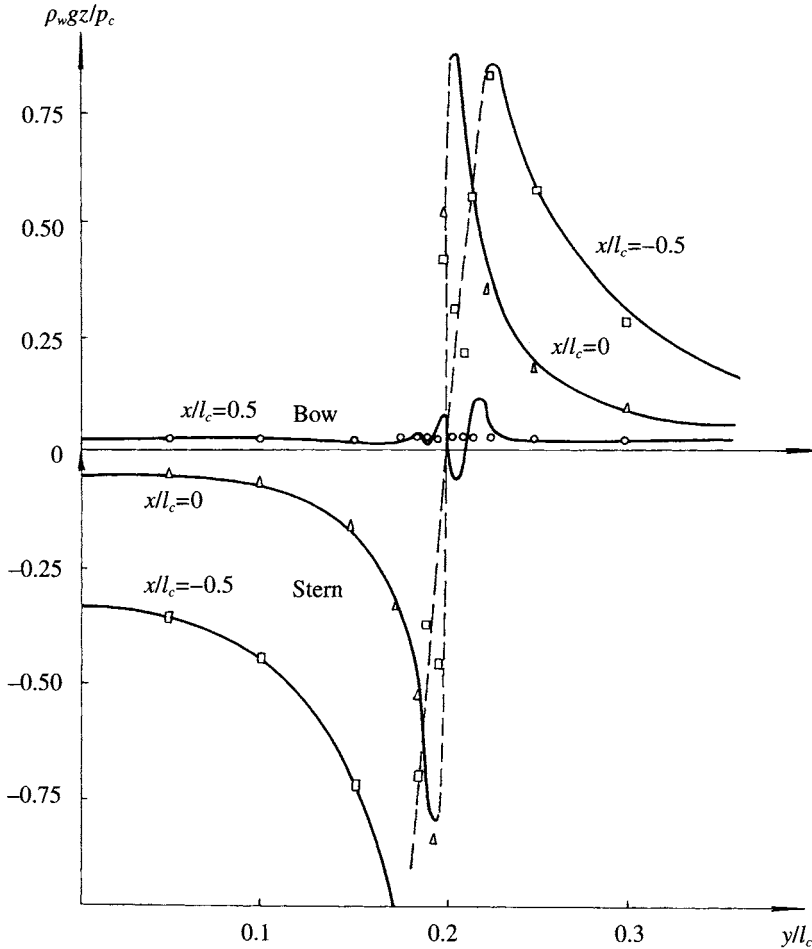


Fig. 5.4 Wave profile in/off cushion due to a moving rectangular air cushion at zero yawing angle and $Fr = 2.12$, $r = 0.4$, where the origin point of co-ordinates is at amidships, bow positives.

2. Behind amidships, particularly at the cushion stern, the water surface descends dramatically at hump speed ($Fn = 0.56$), the depth of depression can reach up to $3-4p_c/\gamma$ (see also Figs 5.5 and 5.2).
3. The height of the water surface changes suddenly from inside the cushion to beyond the cushion (see Figs 5.1 and 5.6). The water surface deformation is also different in the transverse (y) direction.
4. The actual depth of the water surface depression in the cushion is greater than found by calculation (see Fig. 5.6) [54]. This may be due to neglecting viscosity effects of the water as a real fluid and its surface tension, as well as the assumption of linear equations for potential flow in calculation.

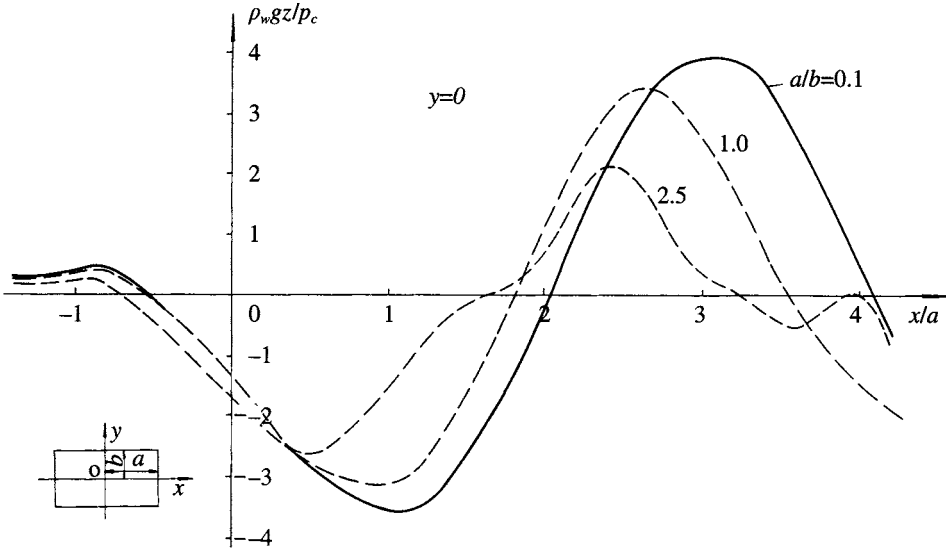


Fig. 5.5 Deformation of water surface of ACV at $Fr = 0.57$ on centreline for different a/b .

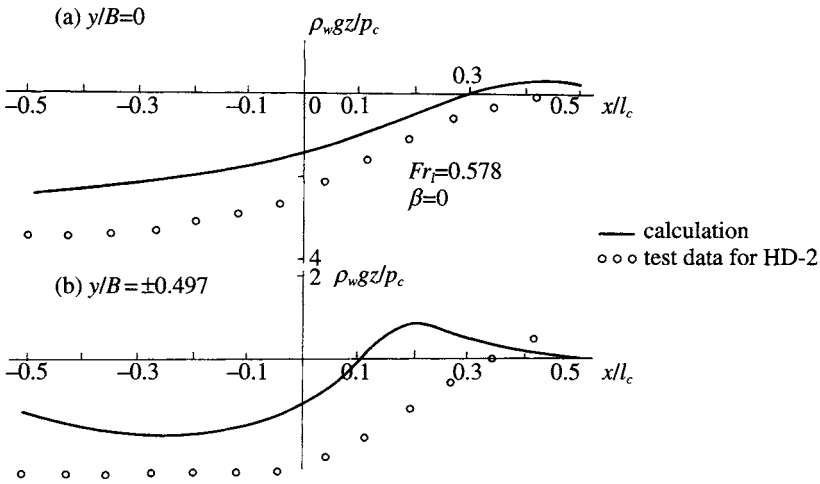


Fig. 5.6 Comparison of water surface deformation of craft HD-2 between calculation and test results. (a) at centreline; (b) in cushion but in close proximity to cushion peripheral boundary.

ACV over shallow water

In shallow water, $\tanh kH$ [53] can be considered as a small value, i.e. $\tanh kH \cong kH$ and $\cosh kH \cong 0$. Then, when $l/H > 10$, the analytical expressions (5.2) can be simplified as

$$\phi = \frac{ip_c}{\pi^2 \rho_w g} \int_{-\infty}^{\infty} \sin \beta r l e^{-i\beta y} \frac{d\beta}{\beta} \int_{-\infty}^{\infty} G da \quad (5.4)$$

where

$$G = \frac{\text{ind. } l e^{i a x}}{H(a^2 + \beta^2) - F n_H^2 a^2 H - i c \mu a l g}$$

$$F n_H = c l (g H)^{0.5}$$

$$\tan \theta = \beta / a$$

$$\gamma = b / l$$

This equation can be developed into an algebraic equation for practical use:

1. When $F n_H > 0$, let

$$\begin{aligned} \mathbf{a} &= (x - l) / [l (F n_H^2 - 1)^{0.5}] \\ \mathbf{b} &= (x + l) / [l (F n_H^2 - 1)^{0.5}] \\ \mathbf{c} &= [\text{sgn}(-\mathbf{a} + r - y/l) + \text{sgn}(\mathbf{a} + r - y/l) + \text{sgn}(-\mathbf{a} + r + y/l) \\ &\quad + \text{sgn}(\mathbf{a} + r + y/l)] \\ \mathbf{d} &= [\text{sgn}(-\mathbf{b} + r - y/l) + \text{sgn}(\mathbf{b} + r - y/l) + \text{sgn}(-\mathbf{b} + r + y/l) \\ &\quad + \text{sgn}(\mathbf{b} + r + y/l)] \\ (\rho w g \eta) / p_c &= [F n_H^2 / (4(F n_H^2 - 1))] \mathbf{c} H(1 - x/l) - \mathbf{d} H(-1 - x/l) \\ &\quad - 0.25 [\text{sgn}((y/l) + r) - \text{sgn}((y/l) - r)] [\text{sgn}((x/l) + 1) \\ &\quad - \text{sgn}((x/l) - 1)] \end{aligned} \quad (5.5)$$

2. When $F n_H < 1$, let

$$\begin{aligned} \mathbf{e} &= \arctan [r/l |x - l| (1 - F n_H^2)^{0.5}] / [(x - l)^2 + (y^2 - r^2 l^2) \\ &\quad (1 - F n_H^2)] \\ \mathbf{f} &= \arctan [r/l |x + l| (1 - F n_H^2)^{0.5}] / [(x + l)^2 + (y^2 - r^2 l^2) \\ &\quad (1 - F n_H^2)] \\ (\rho w g \eta) / p_c &= [F n_H^2 / (2\pi(1 - F n_H^2))] \mathbf{e} \text{sgn}((x/l) - 1) - \mathbf{f} \text{sgn}((x/l) + 1) \\ &\quad - 0.25 [\text{sgn}((y/l) + r) - \text{sgn}((y/l) - r)] [\text{sgn}((x/l) + 1) \\ &\quad - \text{sgn}((x/l) - 1)] \end{aligned} \quad (5.5a)$$

where

$$\text{sgn}(x) = \begin{cases} 1 & \text{when } x > 0 \\ 0 & x = 0 \\ -1 & x < 0 \end{cases}$$

and $H(x)$ is the unit step function.

The wave-making of an ACV running over shallow water can be calculated according to equations (5.5) and (5.5a) in the case where $F n_H = (v/(gH)^{0.5}) > 1$. The maximum height of the wave can be simplified [55] as

$$\begin{aligned} a_0 &= 1/(Fn_H^2 - 1) \\ a_1 &= Fn_H^2 a_0/2 \\ a &= \arctan [1/(Fn_H^2 - 1)^{0.5}] \end{aligned} \quad (5.6)$$

where Fn_H is the Froude number at the particular water depth, v the craft speed (m/s) and H the water depth (m), see Fig. 5.8 below.

The wave-making in/beyond an air cushion running over shallow water can be estimated approximately by means of Fig. 5.7 and equation (5.6). This method is rough, but it is very practical. Figure 5.7 shows the calculation and test results. It may be noticed that theoretical prediction and test results compare well. Figure 5.7 is suitable for conditions where $Fn > 1.38$ and $l/H < 10$, where l denotes the length of air cushion.

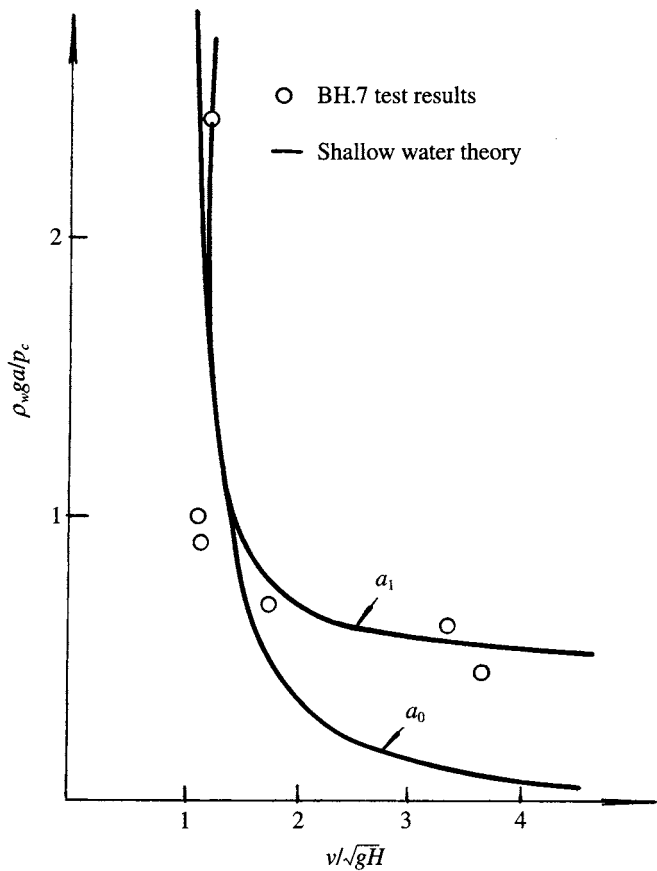


Fig. 5.7 Comparison of non dimensional wave amplitude between the calculation by shallow water wave theory and test results on BH.7.

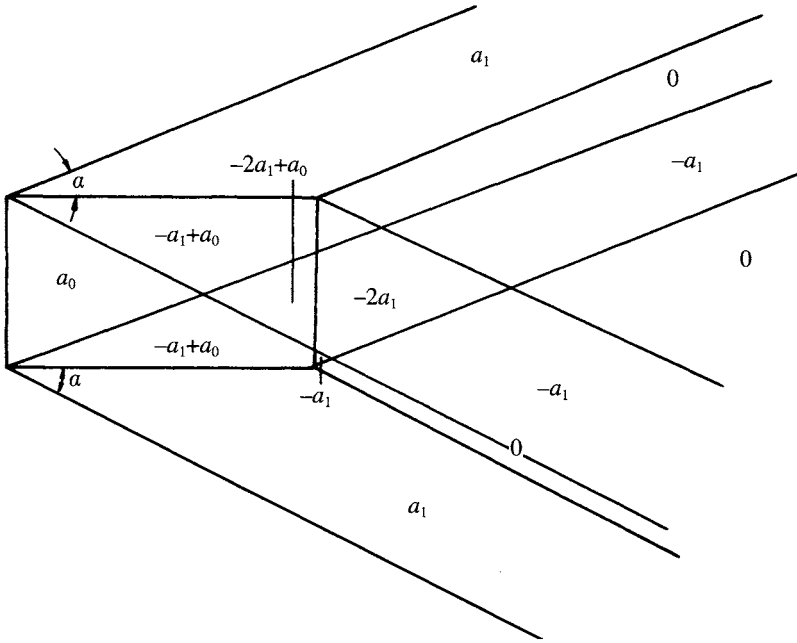


Fig. 5.8 Wave amplitude due to an ACV on shallow water in/off air cushion.

5.3 Water surface deformation in/beyond SES air cushion on calm water

The wave-making of an SES moving on water is different from that of an ACV, resulting from immersion of the two sidehulls in the water. Thus in addition to wave-making induced by the air cushion, the interference of wavemaking between two sidewalls and sidewalls with the air cushion has to be considered.

Based on Standing's formula [54], senior research engineer H. Z. Rong of MARIC developed the wave profile calculation of an ACV into that for an SES [32]. He assumed that the flow around the craft was uniformly distributed, incompressible, non-viscous, with no vortex flow and that the wave height was small with respect to the wave length.

On this basis he established a mathematical model for an SES running at constant speed over water with infinite depth, namely distributed Kelvin sources on the surface of calm water (i.e. the pressure surface at $z = 0$) and on the centre longitudinal plane of both sidewalls (i.e. $r = b$) and also distributed a Kelvin doublet (source/sink) on the surface extending as far as infinity. The coordinate system is as shown in Fig. 5.9.

Using linear water wave theory [56], the equation which defines the disturbing velocity potential and its boundary condition can be obtained and the ϕ broken down into

$$\phi = \phi^P + \phi^R + \phi^L + \phi^M \quad (5.7)$$

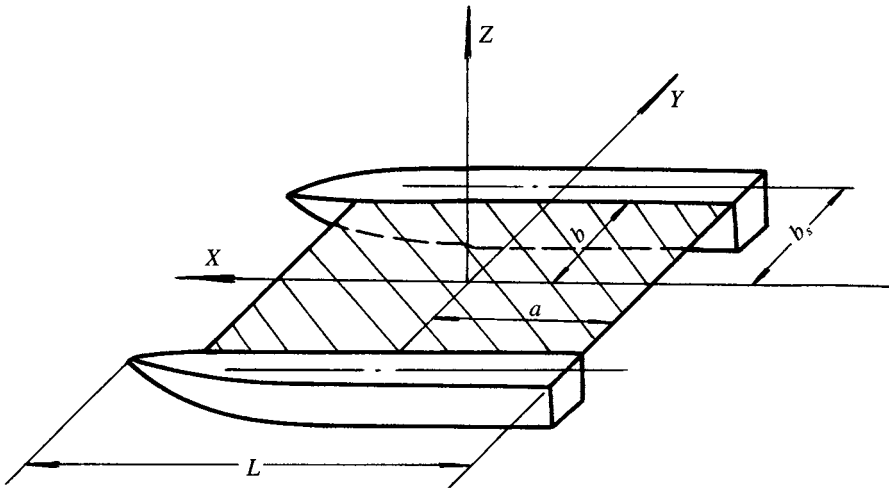


Fig. 5.9 Co-ordinate system and principal dimensions of SES for calculating the inboard/outboard wave profile of SES running on calm water.

where the ϕ^P denotes the distribution of pressure sources on the cushion surface, ϕ^R , ϕ^L the source distribution on the centre longitudinal sidewalls, and doublet ϕ^M the action of interference caused by various factors, each of them meeting the given equations and their boundary conditions. Meanwhile, the amplitude of water surface deformation can also be broken down as follows:

$$\eta = \eta^P + \eta^R + \eta^L + \eta^M \quad (5.8)$$

The terms on the right-hand side in equation (5.8) denote the deformation of the water surface induced by each equivalent source. Figures 5.10 and 5.11 show a comparison of wave profile between calculations and experimental results on the inside ($y = b$) and outside ($y = 1.2b$), of the sidewalls. Experiments were carried out in a towing tank and the results were obtained by analysing photographs. From comparison of the results, MARIC have concluded as follows:

1. The calculated results show that the wave amplitude induced by cushion air pressure is the main component of the total wave height. The wave amplitude induced by interference of both sidewalls and cushion pressure is small relative to the former.

It may be noted that the volume displacement of sidewalls of this craft only occupy 10% of craft displacement. For an air cushion catamaran with wider sidewalls and larger sidewall displacement, the interference effect will increase somewhat. The cushion pressure induced wave components are nevertheless dominant.

The theoretical results generally agree with the tests, which means that the influence of thin sidewalls on the deformation of the water surface induced by cushion air is small.

2. The fluctuations of calculated wave profile (η) shown in Fig. 5.11 may be a reflection of the linear equation used as a mathematical model. In practice the fluctuation can be smoothed by nonlinearity of real water waves and viscosity effects.

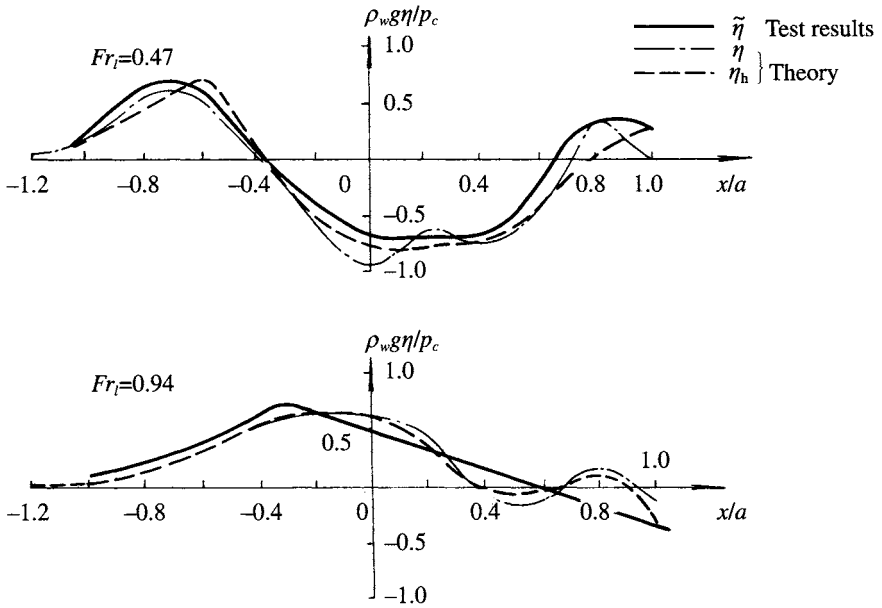


Fig. 5.10 Calculation and experimental results of wave profile at outside of sidewall on model 7205.

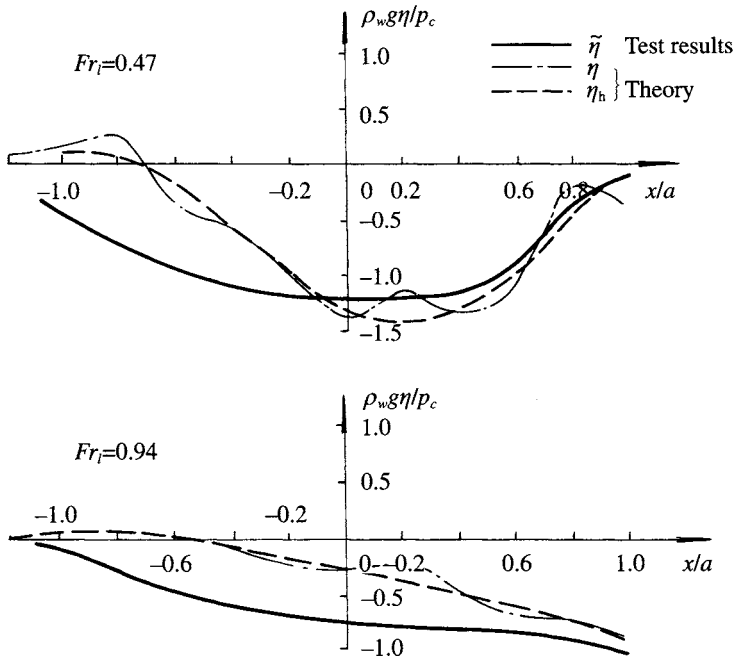


Fig. 5.11 Calculation and experimental results of wave profile at inside of sidewall ($y = b$) on model 7205.

3. In the same way as that in Fig. 5.6 [54], the actual depression in the deformed water surface is deeper than that obtained from calculations.

5.4 Dynamic trim of ACV/SES on cushion over calm water

A theoretical method for predicting ACV/SES dynamic trim over calm water

We take the SES as an example to calculate the dynamic trim. The calculation method predicting the dynamic trim of an ACV on cushion is similar to that of an SES.

Factors determining the dynamic trim of an SES on cushion are numerous, e.g. craft speed (Vn), LCG, configuration of sidewalls, lift fan flow rate and total pressure, cushion length/beam ratio, cushion pressure/length ratio and skirt clearance over the water surface.

The determination of dynamic trim of a craft on cushion has to meet the following conditions:

1. The craft weight must be equal to the sum of buoyancy components and exerting forces, such as lift of air cushion, the static buoyancy and dynamic lift force of sidewalls, the static and dynamic lift force of the bow/ stern seals.
2. The moments of these forces about the CG of the craft must be equal to zero.
3. The inflow and total air pressure of fans must satisfy the air duct characteristic curve and the hovering characteristics of the craft.
4. The water surface elevation (both inboard and outboard of the sidewalls) must follow the wave profiles generated by a uniform distribution of cushion pressure travelling over the calm water at constant speed.

We also make the following assumptions:

1. Owing to the absence of longitudinal and transverse stability keels in the air cushion, the air pressure of the cushion is assumed to be spatially constant, while the craft speed is not very high. This was validated approximately by trials of the craft model 717.
2. Sidewall wave-making effect on dynamic trim and water surface elevation may be neglected.
3. The air cushion is assumed to be incompressible, i.e. the air density in the cushion is constant.

The typical dynamic trim of SES running over calm water on cushion is shown in Fig. 5.12, where we define that:

t_{bo}	=	outer draft of the sidewall at bow
t_{bi}	=	inner draft of the sidewall at bow
t_{so}	=	outer draft of the sidewall at stern
t_{si}	=	inner draft of the sidewall at stern
z_b	=	vertical distance between the lower end of bow seal and baseline
z_s	=	vertical distance between lower end of stern seal and base line
SL	=	sea level
WL _o	=	outer water-line
WL _i	=	inner water-line

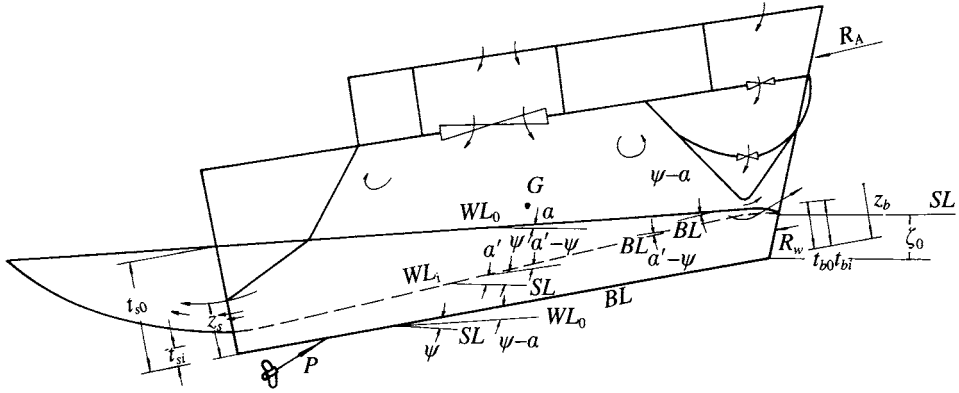


Fig. 5.12 Sketch of running attitude of SES running on calm water.

- a = the slope angle of the outer wave surface to the horizontal plane
- a' = the slope angle of the inner wave surface to the horizontal plane
- ψ = trim angle of craft to the horizontal plane
- $\psi-a$ = apparent trim angle, which can be calculated by the outer water-line
- ζ_0 = vertical distance between the base-line of craft at bow and sea level
- z_{bi} = wave elevation at bow inside cushion
- z_{bo} = wave elevation at bow outer cushion
- z_{si} = wave elevation at stern inside cushion
- z_{so} = wave elevation at stern outer cushion

Then the wave steepness for both inner and outer water-lines can be written as

$$\begin{aligned}
 t_{bi} &= \zeta_0 + z_{bi} \\
 t_{bo} &= \zeta_0 + z_{bo} \\
 t_{so} &= \zeta_0 + z_{bo} + l_c \tan(\psi - a) \\
 t_{si} &= \zeta_0 + z_{bi} - l_c \tan(\psi - a')
 \end{aligned} \tag{5.9}$$

where l_c is the cushion length.

Owing to the small values of ψ , a which are smaller than 5° , the effect on the value mentioned above can be neglected, and the wave steepness for both inner and outer water line can be written as

$$\begin{aligned}
 \tan a &= (z_{so} - z_{bo})/l_c \\
 \tan a' &= (z_{bi} - z_{si})/l_c
 \end{aligned} \tag{5.10}$$

where $\tan a$ is the steepness of the outer wave surface and $\tan a'$ the steepness of the inner wave surface.

Because the elevation of both the inner/outer wave surface can be obtained by the calculation method above the inner/outer draft at bow/stern can be written as

$$t = f(Fn_i, L_c/B_c, p_c/l_c, \psi, \zeta_0) \tag{5.11}$$

where l_c/B_c is the cushion length beam ratio and p_c/l_c the cushion pressure length ratio.

Parameters t_{bi} , t_{bo} , t_{so} , t_{si} can be written as a function of Fn_i , L_c/B_c , P_c/L_c , ψ and ζ_0 , so that the inner/outer sidewall draft of the craft with given principal dimensions and

speed can be obtained as a function of the trim angle and vertical location of bow over sea level.

In order to find ψ and ζ_0 , the other equations to be satisfied are as follows:

$$\begin{aligned}\sum L_i &= W \\ \sum M_i &= 0 \\ H_j &= A + BQ + CQ^2 \\ &= p_c + 0.5\rho_a \sum_{i=1}^n (Q/S_i)^2 \xi_i \\ Q &= (2p_c/\rho_a)^{0.5} \phi A_{es} + (2(p_c - p_v)/\rho_a)^{0.5} \phi A_{eb}\end{aligned}\quad (5.12)$$

in which $\sum L_i$ is the sum of various lift and buoyancy components

$$\sum L_i = L'_c + L_{sw} + L_{ss} + L_{bs} + L_a$$

where L'_c are the lift forces due to the air cushion pressure $L'_c = p_c s_c$, L_{sw} the buoyancy of sidewalls, L_{ss} the lift forces of the stern seal, L_{bs} the lift force of the bow seal and L_a the aerodynamic lift of the superstructure. $\sum M_i$ is the sum of various moments with respect to the CG of the craft

$$\sum M_i = M_c + M_{sw} + M_{ss} + M_{bs} + M_a + M_w + M_p$$

where M_w is the moment of water drag R_w about the CG of the craft, M_a the moment of air drag R_a about the CG of the craft, M_c , M_{sw} , M_{ss} , M_{bs} the moments of L'_c , L_{sw} , L_{ss} , L_{bs} about the CG of the craft and M_p the moment of the propeller thrust about the CG of the craft.

In addition, W is the all-up weight of the craft, H_j the total air pressure of the fans, A , B , C are coefficients of the fan characteristic curve, which are a function of type, dimensions and revolution of fans, ξ_i the air pressure loss coefficients for various air ducts, S_i the area of equivalent air ducts; the calculation for pressure loss of various air ducts in equation (5.12) is hypothetical and one can calculate according to the specific condition. ϕ is the discharge coefficient of air leakage, A_{es} the cross-sectional area of cushion air leakage at the stern, $A_{es} = (z_s - t_{si}) B_c$, A_{eb} the cross-sectional area of cushion air leakage at the bow, $A_{eb} = (z_b - t_{bi}) B_c$ and P_v the ram pressure at bow due to the craft speed v .

Substituting these expressions into equation (5.12), then the four variables ψ , ζ_0 , Q and p_c can be obtained by solving the four equations by iteration. Substitute ψ , ζ_0 into equation (5.11), then the dynamic trim characterized by t_{bo} , t_{bi} , t_{so} , t_{si} , can be obtained.

The method for determining the various forces and moments will be described in following chapters. Solution of these equations is very complicated because this is an iterative process and the forces and moments involved in the equations are a function of inside/outside air cushion conditions and the craft dynamic trim.

The inner/outer drafts are also a function of various forces (moments) and factors of lift systems, e.g. p_c , H_f , Q , but can be easily solved by computer.

This method can also be extended to other parameters for solving the differential equations with respect to stability, heaving, rolling and pitching motions, etc., which will be described in following chapters.

Some important concepts presented in the first section of this chapter, which are often neglected by researchers and designers, may be clarified as follows:

1. The angle calculated by the outer draft of sidewalls at bow and stern is actually the apparent trim angle of the craft (i.e. $\tan(\psi - \alpha) = (t_{so} - t_{bo})/l_c$) and not the true craft trim angle, which often seems misunderstood by some operators. An exception is in the case of high craft speed, when the slope angle of outer wave surface approaches zero, then the apparent trim angle equals the actual trim angle.
2. The trim angle measured by trigonometry (ψ) is the actual trim of the craft.
3. The wave slope of inner water surface α' is related to the cushion wave-making drag and can be written as

$$R_{wc} = W \tan \alpha'$$

This formula is similar to that used for predicting the wave-making drag of a planing hull

$$R_w = W \tan \alpha$$

where R_w is the wave-making drag, W the craft weight and α the wave surface slope (or trim measured by drafts, for a boat).

For an SES the sidehull wavemaking and cushion wavemaking each relate to the proportion of weight supported by displacement and cushion pressure.

4. Trim drag, which is due to the difference of momentum of air leakage from bow and stern skirts, is a function of the slope of the inner water-line and the bow/stern skirt clearance over the base-plane and is directly related to the apparent trim angle ($\psi - \alpha$) and true trim angle ψ .

Therefore it is not correct to estimate the trim drag by this method. The estimation method for trim drag and wave-making drag will be defined in following chapters; however, the concept and method of predicting the dynamic trim of craft, which has been discussed above, is very important to clarify the fundamental relations of the hydrodynamic performance of hovercraft, although the physically correct method is rather more complicated.

Simplified method for predicting hovercraft trim above hump speed on calm water

We assume as follows:

1. The inner/outer water-line may be considered as a straight line because of high craft speed.
2. According to calculation and practical observations, it is found that the inner draft is equal to the outer draft.
3. Owing to the small slope angle of the outer wave surface, we can assume $\alpha \cong 0$ so that $t_{bi} = t_{bo}$ can be added into equation (5.12).

Then because $\alpha \cong 0$ and $t_{bi} = t_{bo}$

$$\begin{aligned} R_w &= W \tan \alpha' \\ &= W \tan [\psi + (\alpha' - \psi)] \end{aligned}$$

$$\begin{aligned}
&\cong W \tan \psi + W \tan (a' - \psi) \\
&\cong W \tan (\psi - a) + W \tan (a' - \psi) \\
&\cong W(t_{so} - t_{bo})/l_c + W(t_{bi} - t_{si})/l_c \\
&\cong W(t_{so} - t_{si})/l_c
\end{aligned} \tag{5.13}$$

From Chapter 4, we have

$$R_w/W = f(Fn_1, l_c/B_c, p_c/l_c) \tag{5.14}$$

Thus equations (5.13) can be used to determine dynamic trim, since the wave-making drag R_w of the given ACV/SES can be estimated and then t_{so} , t_{bo} , t_{si} , t_{bi} , Q , P_{co} , i.e. the dynamic trim of the craft, can be obtained using equations (5.11)–(5.13). The method is so simple that the inner/outer wave profile can be obtained without complicated calculation, as demonstrated in refs 54 and 32.